Evidence for $D^0 - \bar{D}^0$ Mixing using the CDF II Detector

The CDF Collaboration

October 25, 2007

Since the discovery of the charm quark in 1974 [1, 2], physicists have been searching for the oscillation of neutral charm mesons between particle and anti-particle states. More generally, oscillation between a neutral meson and its anti-particle is referred to as "mixing" since the effect can be explained in terms of quantum mechanical mixed states. Mixing was discovered for K^0 mesons in 1964 [3] and for B_d^0 mesons in 1987 [4, 5]. The years 2006 and 2007 have seen landmark new results on mixing: observation of B_s mixing from the CDF II experiment [6] and evidence for D^0 mixing from the BELLE [7] and BaBar [8] experiments.

The recent evidence for D^0 mixing comes from two different types of measurements. The BELLE Collaboration found direct evidence of a longer and shorter lived D^0 meson, in analogy to the well-known case for K^0 mesons. They found significantly different decay time distributions for $D^0 \rightarrow$ CP-eigenstates K^+K^- and $\pi^+\pi^-$ compared to that for $D^0 \rightarrow$ the CP-mixed state $K^-\pi^+$. (In this Letter, reference

to a specific decay chain implicitly includes the charge-conjugate decay.) No other experiment has found evidence for lifetime differences among these decays. The type of evidence for D^0 mixing found in the BaBar experiment was a difference in decay time distribution for $D^0 \rightarrow K^+\pi^-$ compared to that for $D^0 \rightarrow K^-\pi^+$. The difference depends on the combined effects of differences in the masses and lifetimes of the longer-lived compared to the shorter-lived D^0 meson. This same measurement was made in the Belle experiment [9], but no evidence for mixing was seen. In this Letter, we present a measurement comparing the decay time distribution for $D^0 \rightarrow K^+\pi^-$ compared to that for $D^0 \rightarrow K^-\pi^+$.

In the standard model, the decay $D^0 \rightarrow K^+\pi^-$ proceeds through a doubly Cabibbo-suppressed (DCS) "tree" diagram and possibly through a mixing process. The DCS decay rate depends on Cabibbo-Kobayoshi-Maskawa matrix elements as well as the magnitude of SU(3) flavor symmetry violation [11]. Mixing may occur through two distinct types of second-order weak processes. In the first, the D^0 decays into a virtual ("long-range") intermediate state such as $\pi^+\pi^-$, which subsequently decays into a $\overline{D}^0$. The magnitude of the amplitude for long range mixing depends on SU(3) flavor symmetry violation [12]. The second type of second-order weak process is a short range [13], with either a "box" or "penguin" topology. Short range mixing is negligible in the standard model. However, exotic weakly interacting particles could enhance the short range mixing and provide a signature of new physics [14, 15].

The ratio $R(t)$ of $K^+\pi^-$ to $K^-\pi^+$ D^0 decay rates can be expressed [10] as a simple quadratic function of proper time t under the assumption of CP conservation and small values for the parameters x and y. The parameter x is defined in terms of the

mass difference Δm between the heavy and light mass eigenstates and the parameter y involves the mass width difference $\Delta\Gamma$ between these eigenstates according to,

$$x = \Delta m/\Gamma \quad \text{and} \quad y = \Delta\Gamma/2\Gamma$$

where Γ is the average mass width of the mass eigenstates. Under the assumptions stated above,

$$R(t) = R_D + \sqrt{R_D}y't + \frac{x'^2 + y'^2}{4}t^2. \tag{1}$$

The parameters x' and y' are linear combinations of x and y according to the relations,

$$x' = x \cos \delta + y \sin \delta \quad \text{and} \quad y' = -x \sin \delta + y \cos \delta$$

where δ is a strong interaction phase.

The best previous measurements of R_D, y', and x'^2 are from the BELLE and BaBar experiments and are presented in Table 1 (along with the results of this measurement which will be discussed later).

Our measurement uses data collected by the CDF II detector at the Fermilab Tevatron collider, from October 2002 to January, 2007. The data set corresponds to an integrated luminosity of 1.5 fb^{-1} with $\bar{p}p$ collisions at $\sqrt{s} = 1.96$ TeV. CDF II is a multi-purpose detector with a magnetic spectrometer surrounded by a calorimeter and a muon detector.

To study D^0 mixing, we reconstruct the Cabibbo-favored decay chain $D^{*+} \to \pi^+ D^0$, $D^0 \to K^- \pi^+$, called "right sign" (RS) and we reconstruct $D^{*+} \to \pi^+ D^0$,

Table 1: Comparison of the CDF II result for charm mixing parameters with recent measurements. All results use $D^0 \to K^+\pi^-$ decays and fits assuming no CP violation. The uncertainties include statistical and systematic components. The significance for non-zero mixing is given in terms of the equivalent Gaussian standard deviation. For CDF II, the correlation coefficient between y' and x'^2 is -0.98. The fits assume no CP violation.

Expt.	$R_D(10^{-3})$	$y'(10^{-3})$	$x'^2(10^{-3})$	Signif.
CDF II	3.04 ± 0.55	8.5 ± 7.6	-0.12 ± 0.35	3.8
BaBar [8]	3.03 ± 0.19	9.7 ± 5.4	-0.22 ± 0.37	3.9
Belle [?]	3.64 ± 0.17	$0.6\,{}^{+4.0}_{-3.9}$	$0.18\,{}^{+0.21}_{-0.23}$	2.0

$D^0 \to K^+\pi^-$, called "wrong-sign" (WS). The reconstruction method is similar to that used in our recent measurement [16] of the time-integrated ratio of WS to RS decay rates.

We choose off-line analysis cuts to maximize the significance of the WS signal determined from a study of the RS signal and the WS background. We optimize the cuts without using WS candidates and before the candidates are revealed. To estimate the WS signal, we scale the RS signal by the world average for R_D. To estimate the WS background, we use candidates in a control region of D^* invariant mass, outside a region containing the signal. To reduce systematic uncertainty, we use the same set of cuts for both the RS and WS decay modes.

The D^0 candidate reconstruction starts with a pair of oppositely charged tracks that satisfy the trigger requirements. The tracks are considered with both $K^-\pi^+$ and π^-K^+ interpretations. A third track, which is required to have $p_T \geq 0.3$ GeV/c, is used to form a D^* candidate when combined as a pion with the D^0 candidate. The

charge of this "tagging pion" determines whether the D^0 candidate decay is RS or WS.

We apply two cuts to reduce the background to the WS signal from RS decays where the D^0 decay tracks are mis-identified because the kaon and pion assignments are mistakenly interchanged. This background is characterized by a $K\pi$ mass distribution with width about ten times that of the signal peak. A WS candidate that is consistent with being a RS decay, with $K^-\pi^+$ invariant mass within $\pm$ 20 MeV/c^2 of the D^0 mass, is excluded. This cut rejects 97.5% of mis-identified decays, while retaining 78% of the signal. Since the analysis procedure is the same for WS and RS decays, a RS candidate that is consistent with being a WS decay is excluded from the RS signal. We also employ a cut based on particle identification (PID) from specific ionization in the COT which helps to reject mis-identified decays, but with a smaller improvement to WS signal significance than from the cut based on invariant mass. This PID cut is described in [16] and utilizes the PID information from all three tracks in the decay chain.

To determine the signal and background, RS and WS candidate events are divided into bins of proper decay time, D^* mass difference ($\Delta m = m(K\pi\pi) - m(K\pi) - m(\pi)$), and $K\pi$ mass. The $K\pi$ mass distribution is fit using a binned likelihood method with a double Gaussian shape for D^0 signal and a quadratic function for the background. An example is given in figure 1. The number of D^0 events is determined for each bin of mass difference. The mass difference distribution is fit with a least-squares method with a D^* signal shape and a power function (Δm^A) for the background from D^0s that form fake D^* candidates. Examples for the mass difference fits are given in

5

figure 2 for Right-Sign and figure 3 for Wrong-Sign.

The decay length is measured from the primary vertex. Some of the D^*s come from B decays, which will result in an incorrect measured decay time. Figure 4 shows the impact parameter distribution for the D^*s, which is part of the information used to calculate the correction due to B decays.

The ratio of wrong-sign to right-sign (corrected) D^*s is determined for the twenty decay time bins. The distribution is fit with a parabola, which is related to the mixing parameters by equation 1. Figure 5 has the results of the fit.

The uncertainty on the mixing parameters includes effects from statistical fluctuations, uncertainties from the signal and background shapes, and the correction due to charm mesons from B decays. We considered other sources of systematic uncertainty, which were negligible compared to the uncertainties listed. Many of the uncertainties for RS and WS fits are common to both, and do not affect the WS/RS ratio.

A Bayesian method is used to get the probability for different mixing parameter values. Contours containing the highest probability points are shown in figure 6. The no-mixing point ($y' = x'^2 = 0$) lies outside the contour equivalent to 3.8 standard deviations, which is evidence for charm mixing.

References

[1] J.J. Aubert *et al.*, Phys. Rev. Lett. **33**, 1404 (1974).

[2] J.E. Augustin *et al.*, Phys. Rev. Lett. **33**, 1406 (1974).

[3] J.H. Christenson *et al.*, Phys. Rev. Lett. **13**, 138 (1964).

[4] C. Albajar *et al.* (UA1 Collaboration), Phys. Lett. B **186**, 247 (1987).

[5] H. Albrecht *et al.* (ARGUS Collaboration), Phys. Lett. B **192**, 245 (1987).

[6] A. Abulencia *et al.* (CDF Collaboration), Phys. Rev. Lett. **97**, 242003 (2006).

[7] M. Starič *et al.* (BELLE Collaboration), Phys. Rev. Lett. **98**, 211803 (2007).

[8] B. Aubert *et al.* (BaBar Collaboration), Phys. Rev. Lett. **98**, 211802 (2007).

[9] L. M. Zhang *et al.* (Belle Collaboration), Phys. Rev. Lett. **96**, 151801 (2006).

[10] B. Aubert *et al.* (BaBar Collaboration), Phys. Rev. Lett. **91**, 171801 (2003).

[11] M. Gronau and J. L. Rosner, Phys. Lett. B **500**, 247 (2001).

[12] A. F. Falk *et al.*, Phys. Rev. D **69**, 114021 (2004).

[13] E. Golowich and A. A. Petrov, Phys. Lett. B **625**, 53 (2005).

[14] G. Burdman and I. Shipsey, Annu. Rev. Nucl. Sci. **53**, 431 (2003). See section 2.3.

[15] E. Golowich, S. Pakvasa and A. A. Petrov, Phys. Rev. Lett. **98**, 171801 (2007).

[16] A. Abulencia et al. (CDF Collaboration), Phys. Rev. D 74, 031109(R) (2006).

[17] D. Acosta *et al.* (CDF Collaboration), Phys. Rev. D **71**, 032001 (2005).

[18] A. Sill *et al.*, Nucl. Instrum. Methods **A447**, 1 (2000).

[19] T. Affolder *et al.*, Nucl. Instrum. Methods **A526**, 249 (2004).

[20] E. J. Thomson *et al.*, IEEE Trans. Nucl. Sci. **49**, 1063 (2002).

[21] W. Ashmanskas *et al.*, Nucl. Instrum. Methods **A518**, 532 (2004).
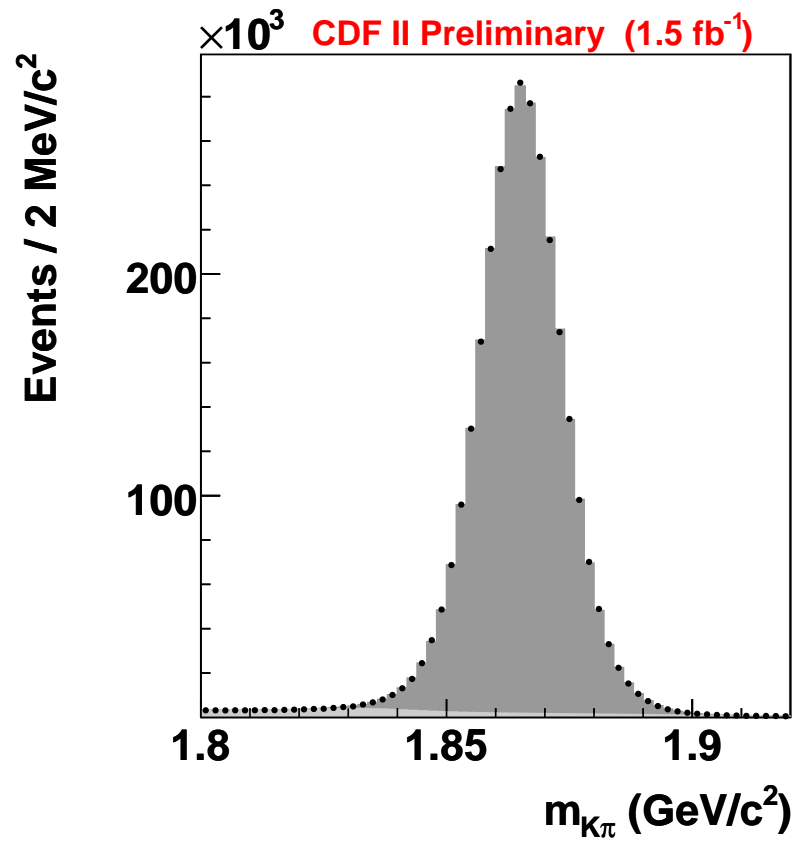
Figure 1: Example $K\pi$ distribution of "right-sign" D^0 candidates. The candidates are required to have a mass-difference between 3-9 MeV.
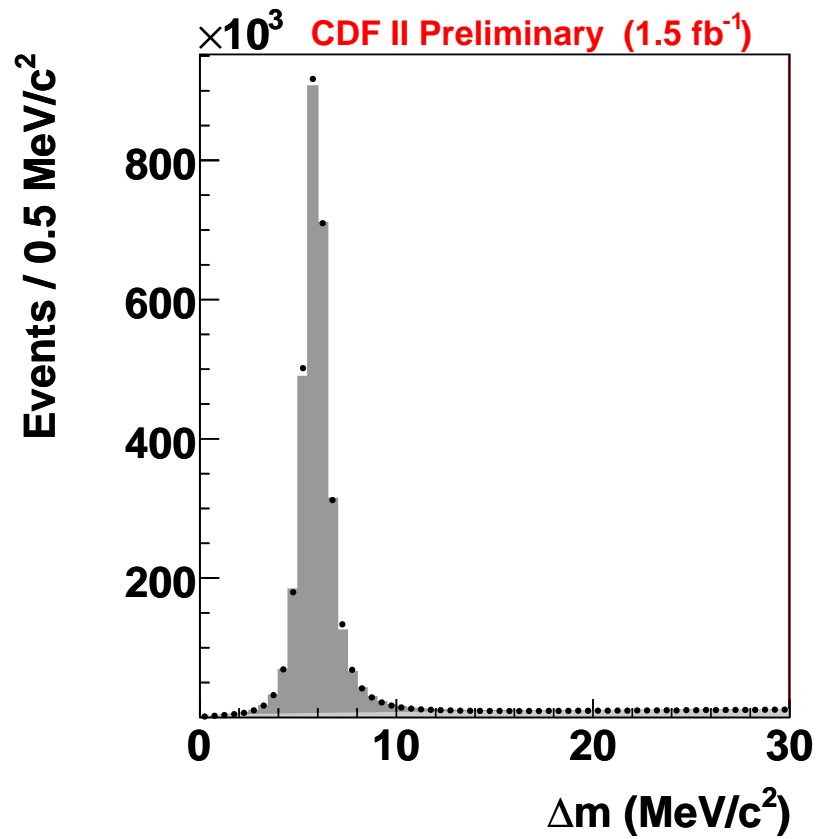
Figure 2: Example mass difference distribution for "right-sign" D^* candidates. The number of D^0s in each bin are the result of 60 separate $K\pi$ fits.
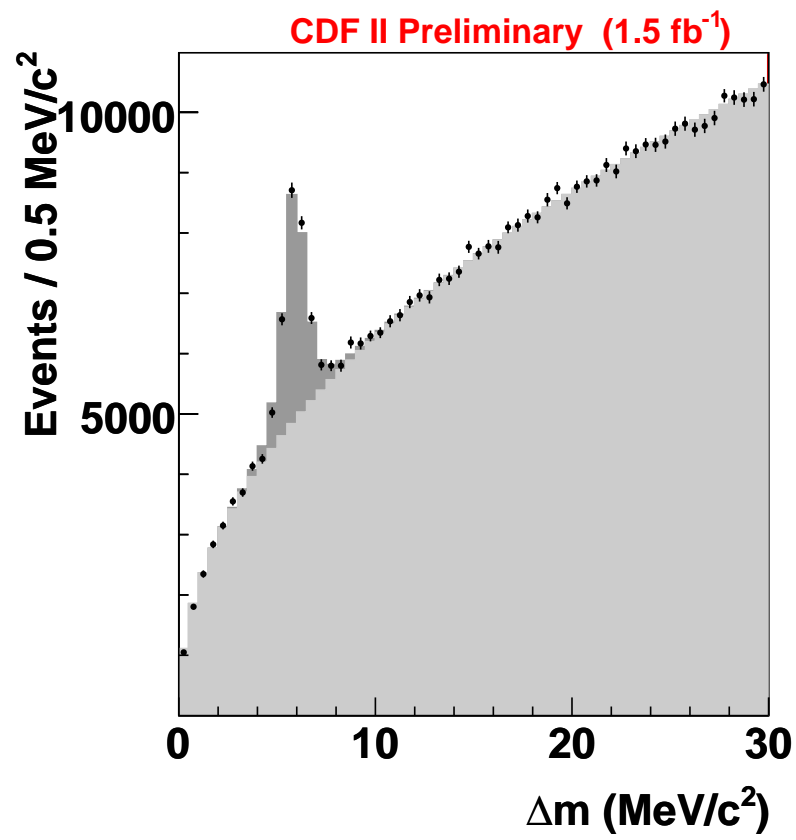
Figure 3: Example mass difference distribution for "wrong-sign" D^* candidates.
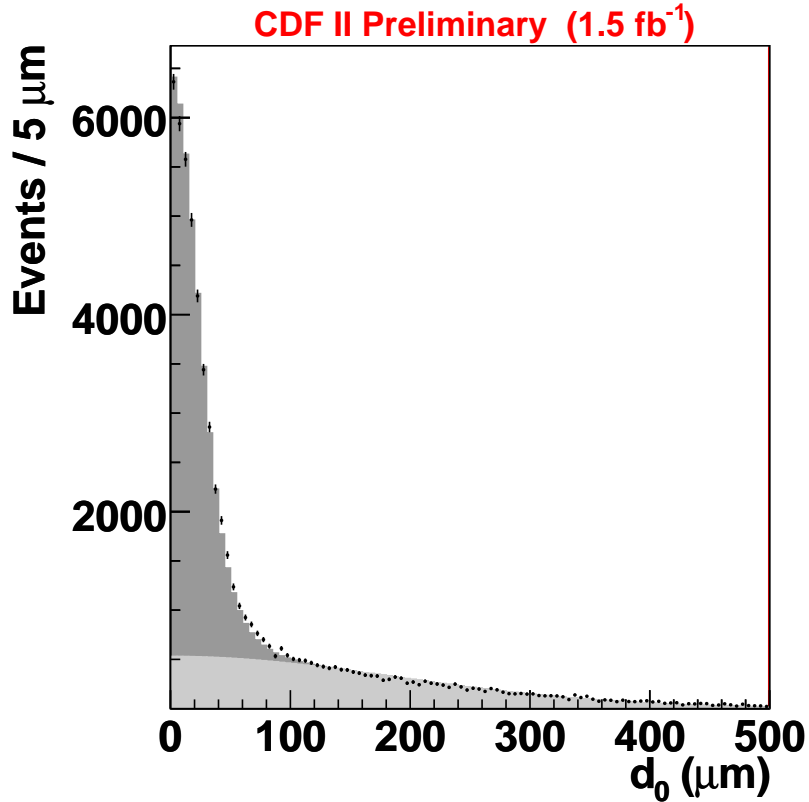
Figure 4: Example distribution of transverse impact parameter d_0 of the "right-sign" D^0 candidate with respect to the primary vertex for $5 < t < 6$. The narrow peak is due to promptly produced D^0 mesons and the broad distribution is due to non-prompt D^0 mesons from B decay. The result of a binned maximum likelihood fit shows the prompt (dark shaded) and non-prompt (light shaded) contributions. The D^* signal region for this figure is $4 < \Delta m < 9$ MeV/c^2, and the D^0 signal region is $1.850 < m_{K\pi} < 1.878$ GeV/c^2. The combinatoric background (about 2% of the signal) is removed using d_0 distributions from the sideband regions, $1.800 < m_{K\pi} < 1.824$ GeV/c^2 and $1.904 < m_{K\pi} < 1.918$ GeV/c^2.
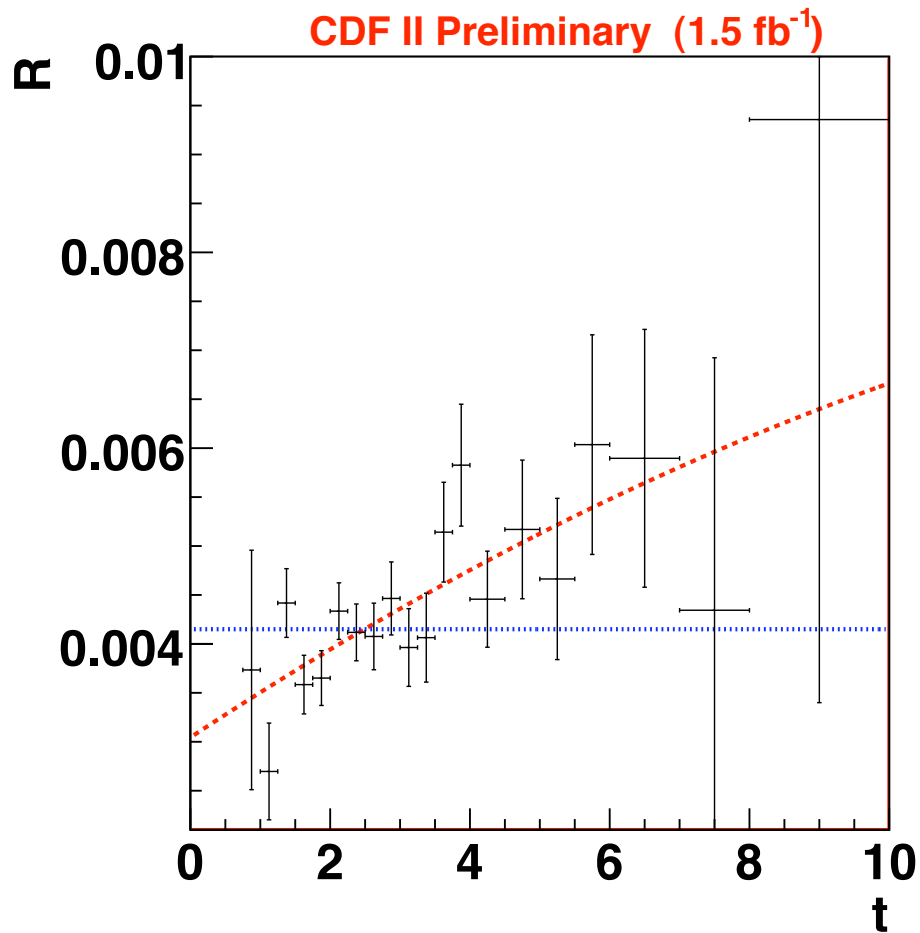
Figure 5: Ratio of prompt D^* "wrong-sign" to "right sign" decays as a function of normalized proper decay time. The dashed curve is from a least-squares quadratic fit. The parameters R_D, y', and x'^2 are determined from this fit. The dotted line is the best fit if we assume no mixing.
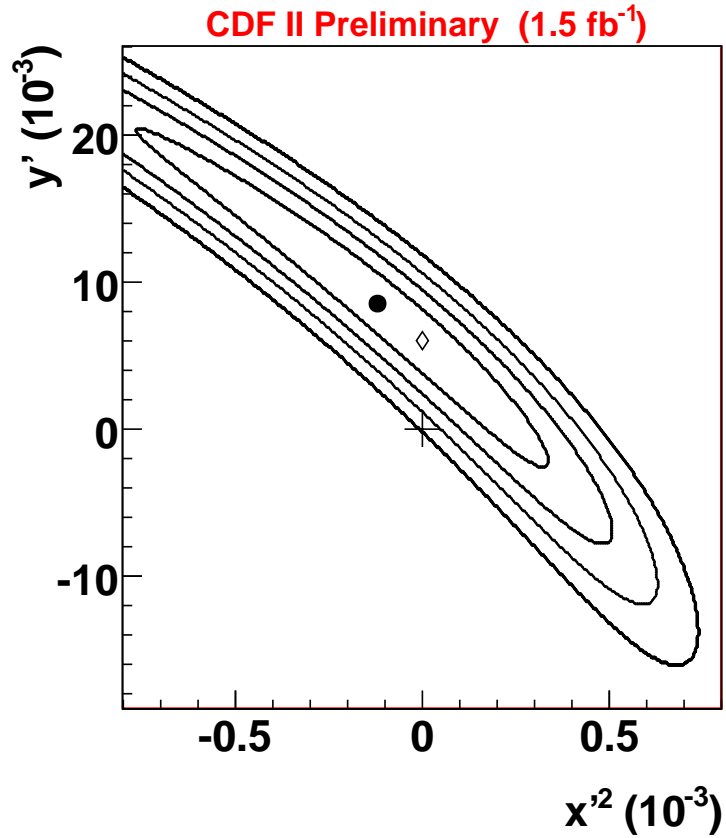
Figure 6: Bayesian probability contours in the $x'^2 - y'$ parameter space corresponding to one through four equivalent Gaussian standard deviations. The closed circle is the best fit value for the mixing parameters. The open diamond is the highest probability point that is physically allowed ($x'^2 \geq 0$). The cross is the no-mixing point.